POLITECNICO DI TORINO
Repository ISTITUZIONALE

Automated mode tracking via supervised classification and adaptive parameter calibration for seismic monitoring with sparse sensors

Original
Automated mode tracking via supervised classification and adaptive parameter calibration for seismic monitoring with sparse sensors / Coccimiglio, S., Miraglia, G., Cavanni, V., Crocetti, A., Ceravolo, R.. - In: BULLETIN OF EARTHQUAKE ENGINEERING. - ISSN 1570-761X. - ELETTRONICO. - 23:10(2025), pp. 4091-4117. [10.1007/s10518-025-02196-9]

Availability:
This version is available at: 11583/3000987 since: 2025-06-16T14:22:44Z

Publisher:
Springer

Published
DOI:10.1007/s10518-025-02196-9

Terms of use:

This article is made available under terms and conditions as specified in the corresponding bibliographic description in the repository

Publisher copyright

(Article begins on next page)

18 November 2026

Bulletin of Earthquake Engineering
https://doi.org/10.1007/s10518-025-02196-9

ORIGINAL ARTICLE

Automated mode tracking via supervised classification and adaptive parameter calibration for seismic monitoring with sparse sensors

Stefania Coccimiglio[1] · Gaetano Miraglia[1,2] · Valeria Cavanni[1] · Alessio Crocetti[1,2] · Rosario Ceravolo[1,2]

Received: 25 February 2025 / Accepted: 31 May 2025
© The Author(s) 2025

Abstract
One of the most important issues to address in the practical implementation of permanent dynamic Structural Health Monitoring (SHM) systems is undoubtedly that of Mode Tracking (MT). Indeed, the influence of environmental and random fluctuations, as well as the uncertainty inherent in the identification algorithms themselves, especially the spill-over effects linked to unmodeled dynamics, can make it difficult to disentangle the various modal behaviours. This separation process, i.e the MT procedure, involves comparing vibration mode estimates with a reference set of modal properties. Although this operation can be straightforward for simple structures, in many practical applications of structural engineering, when there is strong modal concentration (e.g. lattice structures) or high geometric and mechanical complexity (e.g. monumental buildings) greater challenges arise, which grow in the presence of sparse sensor setups (civil structures in general), the superposition of exogenous frequency components (industrial structures, bell towers etc.) and environmental fluctuations. This study presents an innovative MT methodology that combines supervised classification, using advanced machine learning algorithms, with adaptive multi-threshold calibration to overcome the limitations of current MT techniques. The approach incorporates clustering analysis to characterize vibration modes by their natural frequencies and mode shapes, ensuring accurate identification and rejection of spurious data. The method was validated with a simplified numerical model and then demonstrated on a baroque monumental structure equipped with a long-term monitoring system. In addition to being efficient and robust compared to traditional techniques, the proposed procedure is effective for automating the monitoring of modal parameters in SHM systems, even in scenarios with limited sensor deployments.

Keywords Structural Health Monitoring · Long-Term monitoring · Monumental Buildings · Sparse sensors configuration · Mode Tracking · Frequency Domain Decomposition

Extended author information available on the last page of the article

Published online: 16 June 2025

1 Introduction

Mode Tracking (MT) plays a critical role in assessing the structural integrity of essential infrastructure, large structures, and monumental buildings (Rainieri et al. 2012; Ubertini et al. 2016; Nicola Cavalagli and Ubertini 2018). As a key component of SHM, MT provides valuable insights into the dynamic behaviour of structures, essential for evaluating their condition and predicting potential failures. Vibration modes, which are sensitive indicators of structural health, can change due to many factors, including structural damage, loading conditions, and environmental variations. In particular, Environmental and Operational Variations (EOVs) correspond to physiological phenomena that are often mistaken for signs of damage and, in more severe cases, may even mask the presence of actual structural damage, thereby compromising the effectiveness of monitoring activities (Sohn et al. 2002; Limongelli 2019b). Numerous studies highlight the effects of EOVs on vibration-based damage detection (Cawley 1997; Ruotolo and Surace 1997; Sohn et al. 2002; Moser and Moaveni 2011; Ceravolo et al. 2021). During the identification phase, it is not always clear which natural frequency corresponds to each identified vibration mode. MT addresses this by coupling each natural frequency to its corresponding mode over time, enabling continuous monitoring and early detection of potential issues. This allows for timely interventions that can prevent catastrophic failures. MT is commonly achieved by comparing estimated natural frequencies and their associated mode shapes with a set of reference vibration modes (Pereira et al. 2022), thus involving the comparison of new experimental data with the baseline defined at the beginning of the process. Regarding the definition of the set of the reference modes, it can be established from a specific experimental campaign conducted under well-defined conditions (Dederichs and Øiseth 2024) or by an identification obtained from long-term monitoring acquisitions. An alternative approach involves defining the baseline as statistics from clusters identified through multiple acquisitions over time, reflecting the overall behaviour of the structure as external conditions vary. Once the baseline is defined, the focus must then be directed towards selecting the appropriate algorithm. Recently, emphasis has been placed on automating and optimizing MT algorithms, as traditional methods often require extensive manual intervention, making the process time-consuming and error-prone, indeed manual tracking can also lead to inconsistencies in interpreting modal parameters. In addition, it is important to emphasize that this process becomes increasingly complex as structures become more complex and are monitored with fewer sensors (González and Boroschek 2020). In the case of automated MT algorithms, they are based on various parameters that have to be calibrated to perform tracking effectively. Thus, thresholds are established to accept or exclude certain natural frequency values, which can be determined using different criteria and parameters, such as the Modal Assurance Criterion (MAC) and frequency values (Magalhães et al. 2009), only MAC values (Coccimiglio et al. 2023), or other (Brehm et al. 2010; González and Boroschek 2020). Given the importance of MT, research increasingly aims to automate and reduce reliance on human decision-making, minimizing potential errors. Recent advancements in MT algorithms focus on enhancing both robustness and adaptability, ensuring that algorithms can track modal parameters throughout a structure lifecycle while accommodating the diverse dynamic features of different structures. In literature, there are several studies with the aim to define efficient and robust MT algorithms. (Dederichs and Øiseth 2024) introduce a near-automatic MT algorithm for large civil infrastructure, such as bridges, using Operational

Modal Analysis (OMA) data without human intervention. It has been successfully applied to real-world structures like the Hardanger suspension bridge and Bergsøysund floating pontoon bridge. (Brehm et al. 2010) propose an Energy-based Modal Assurance Criterion (EMAC) to improve mode assignment in Finite Element Model (FEM) updating, especially when dealing with incomplete spatial data and noise. (Diord et al. 2017) present an automated system for detecting small structural changes in a stadium roof by tracking modal parameters, filtering out environmental and operational effects over a four-year monitoring period. (Yang et al. 2022) implement a fully automated MT procedure for long-span high-speed railway bridges, identifying modal parameters under varying loads to ensure safety and performance. (Sivori et al. 2024) present a MT approach for nine masonry buildings within the Seismic Observatory of Structures (OSS), each equipped with a range of 11 to 30 sensors. They extend a method based on the Frequency Domain Decomposition (FDD) technique to track the natural frequencies of the buildings over time. Their main goal is to investigate the influence of environmental variables on natural frequencies, a topic of significant debate in SHM (Ubertini et al. 2017). Given the high number of sensors deployed in these buildings, the FDD technique proves particularly well-suited for natural frequency tracking. However, this technique may become not suitable in situations where only a limited number of sensors can be deployed, such as in the case of historical or monumental buildings, where installing numerous sensors is often not feasible. In fact, (González and Boroschek 2020) demonstrate in their study that while a reduced number of sensors can capture the lower modes, identifying the higher modes becomes more problematic. To address this, they present various methods using different numbers of sensors and show that the FDD method is ineffective when few sensors are used. (Cabboi et al. 2017) present the effectiveness of an automated MT procedure using self-adaptable thresholds for permanent dynamic monitoring of the San Michele iron arch bridge. Their method successfully identified and tracked modal properties over time without manual threshold adjustments.

In light of these developments, this study introduces an innovative and reliable methodology for MT in complex structures monitored with sparse sensor configurations (Scussolini et al. 2023; Ceravolo et al. 2024). The approach integrates a scaled representation of modal shapes with advanced clustering analysis, starting from natural frequencies and mode shapes identified using a Stochastic Subspace Identification (SSI) algorithm. In this process, the identified mode shapes are scaled by their associated frequencies to form a scaled mode shapes space, which incorporates both frequency values and mode shapes, with dimensions corresponding to the sensor setup (i.e., number of channels of acquisition). By leveraging prior experimental knowledge of the structure, modes are clustered around known frequency values and mode shapes, ensuring accurate mode identification and tracking. The methodology combines supervised classification, adaptive parameter calibration, and outlier rejection to refine the extracted data, resulting in more accurate and robust outcomes compared to traditional methods, which often face challenges with data coming from sparse sensor configurations. Applied to a complex historical masonry structure monitored by a long-term system with three accelerometers, this approach ensures efficient and reliable tracking of natural frequencies, even with limited sensor configurations.

The paper is organized as follows: Section 2 introduces the proposed MT algorithm, while Section 3 shows its numerical application on a simplified Multi-Degree of Freedom (MDoF) system. In Section 4, the MT method is applied to a full-scale monitored structure,

and its results are compared with those obtained using the FDD method. This is followed by the presentation of the classifier outcomes. Finally, Section 5 provides the conclusions.

2 Tracking modal parameters from permanent monitoring

2.1 Supervised classification analysis

The method here proposed for the MT of frequency time histories requires, starting from the frequencies and mode shapes obtained through a SSI algorithm, a preliminary clustering analysis. In order to support the partitioning of the feature space, in this phase all the identified mode shapes are pre-multiplied by their natural frequency to find a final space representation which, being properly scaled for clustering, reveals the main direction of motion of the mode under analysis (e.g., mainly longitudinal, or mainly transversal). Such space can be defined as *scaled mode shape space* and its dimension depends on the number of accelerometers of the designed setup configuration. Indeed, if three accelerometers are positioned to record the dynamic response of a structure, two in Y direction ($y1$ and $y2$) and one in X direction ($x1$), the final space representation will be 3-dimensional. In detail, the identified mode shape belonging to the k^{th} mode is given by $\mathbf{\Phi}_k = [\phi_{k,y1},\ \phi_{k,x1}, \phi_{k,y2}]$, where $\phi_{k,y1},\ \phi_{k,x1}, \phi_{k,y2}$ are the coordinates of the identified eigenvector associated with the $y1$, $x1$, and $y2$ degrees of freedom, respectively. The identified mode shape $\mathbf{\Phi}_k$ is then multiplied by the corresponding natural frequency f_k, resulting in the *scaled mode shape* vector $f_k\mathbf{\Phi}_k = [f_k\phi_{k,y1},\ f_k\phi_{k,x1}, f_k\phi_{k,y2}]$. Then, exploiting the knowledge from a previous experimental campaign developed on the analysed structure, a clustering of each class k of vibrational modes is performed. Indeed, if the main direction of motion and a mean value of the associated natural frequency are known, the data belonging to the k^{th} mode are clustered around the known natural frequency values and along the main direction of motion in the scaled mode shapes space. Since this procedure could be affected by the user sensitivity, the values of the natural frequencies and of the mode shapes classified as the mode k in each recorded signal are averaged between them to find at most one value of frequency, f_k, and one mode shape, $\mathbf{\Phi}_k$, for each mode k in each recorded signal. Then, the f_k and the $\mathbf{\Phi}_k$ identified for the first recorded signal are respectively mediated with the f_k and the $\mathbf{\Phi}_k$ of the consequent recorded signal, to obtain one value of f_k and one vector $\mathbf{\Phi}_k$ for each couple of recorded signals. In the specific case in which a mode has been identified only in one of the two signals, those identified values are considered as representative of the signals couple. This procedure is applied to each mode class k. These averaged quantities are then cleaned with an adaptive parameters calibration to remove outliers. From the cleaned data two machine learning models are obtained for a fast classification of the future identifications. Within this work application, Support Vector Machines (SVM), according to (Cortes and Vapnik 1995), have been chosen in the supervised classification procedure. When labels are available, i.e. information on the k^{th} mode for the corresponding $\mathbf{\Phi}_k$, the algorithm can learn a relationship among them in a model development aimed at applying this knowledge to fresh data, whose information (label) is unknown. In the context of supervised learning, a classification problem emerges when a dataset is presented, either one-dimensional or multi-dimensional, and the objective is to assign to each data a specific label from a predefined set of categorical classes, which are presented as discrete. For example, for a

modal identification, they are generally represented by the number of mode class k. The available features and corresponding labels are used to initialise the algorithm, described by SVM. In particular, data is partitioned in a training, validation and testing dataset. Within the model generation, training and validation datasets are exploited: the reason why this last is employed is to be addressed at overfitting avoidance, i.e. failing at generalizing new data due to the too tightly adaptation to the training dataset. The testing dataset is described by unseen data, whose labels are questioned at the classification model, giving as input data only its features, represented by $f_k \mathbf{\Phi}_k$, whose k is unknown, or it could not describe a structural mode at all (outliers). In this application, the Statistics and Machine Learning Toolbox (MATLAB®) has been exploited with the purpose of generating two classification models: an optimizable and a linear SVM for which the validation datasets are assumed five-fold cross validated. Finally, to establish the performance of the algorithm used in the classification process, the accuracy (Eq. 1), a metric constructed from the number of True Positives (TP), False Positives (FP), True Negatives (TN) and False Negatives (FN) is defined as:

$$\text{Accuracy} = \frac{\text{TP} + \text{TN}}{\text{TP} + \text{TN} + \text{FP} + \text{FN}} \tag{1}$$

2.2 Adaptive Parameter Calibration

Existing MT approaches often fail in scenarios where modes are closely spaced in frequency or when a limited number of sensors are available to estimate the eigenvectors (González and Boroschek 2020). The proposed approach overcomes this limitation by introducing an optimization-based MT framework that systematically minimizes time bifurcations while ensuring dense data classification. This is achieved by calibrating two thresholds for each reference vibrational mode (or class), un-constraining the problem from the need to assign a single threshold to the all set of reference modes and by integrating a term in the cost function that considers the potential time bifurcation in tracked time histories. This ensures that each tracked vibrational mode remains statistically consistent over time. Figure 1 present the flow chart of the proposed method. Once the classification phase is finished, the next step is to proceed with the tracking of the frequency time series over time. When dealing with MT of complex structures, where the modes can be very close to each other, using a single parameter to define the time series may not be sufficient. In these cases, it is much more convenient to use multiple thresholds parameters with automatic adaptive procedures.

This type of procedure is able to find the optimal values of the thresholds in order to track the correct time history of the natural frequencies. In this study, two parameters are used, the MAC error (e_{MAC}) (Eq. 2) (Bohle and Fritzen 2003; Cabboi et al. 2017) and frequency error (e_{freq}) (Eq. 3)(Bohle and Fritzen 2003; Cabboi et al. 2017), defined as follows:

$$e_{MAC} = 1 - MAC \tag{2}$$

$$e_{freq} = \left| \frac{f_{ref} - f}{f_{ref}} \right| \tag{3}$$

In Eq. 3, f_{ref} is referred to as the set of reference modes, defined as the average of the values of each cluster; while f is the natural frequency, so the frequency error is computed

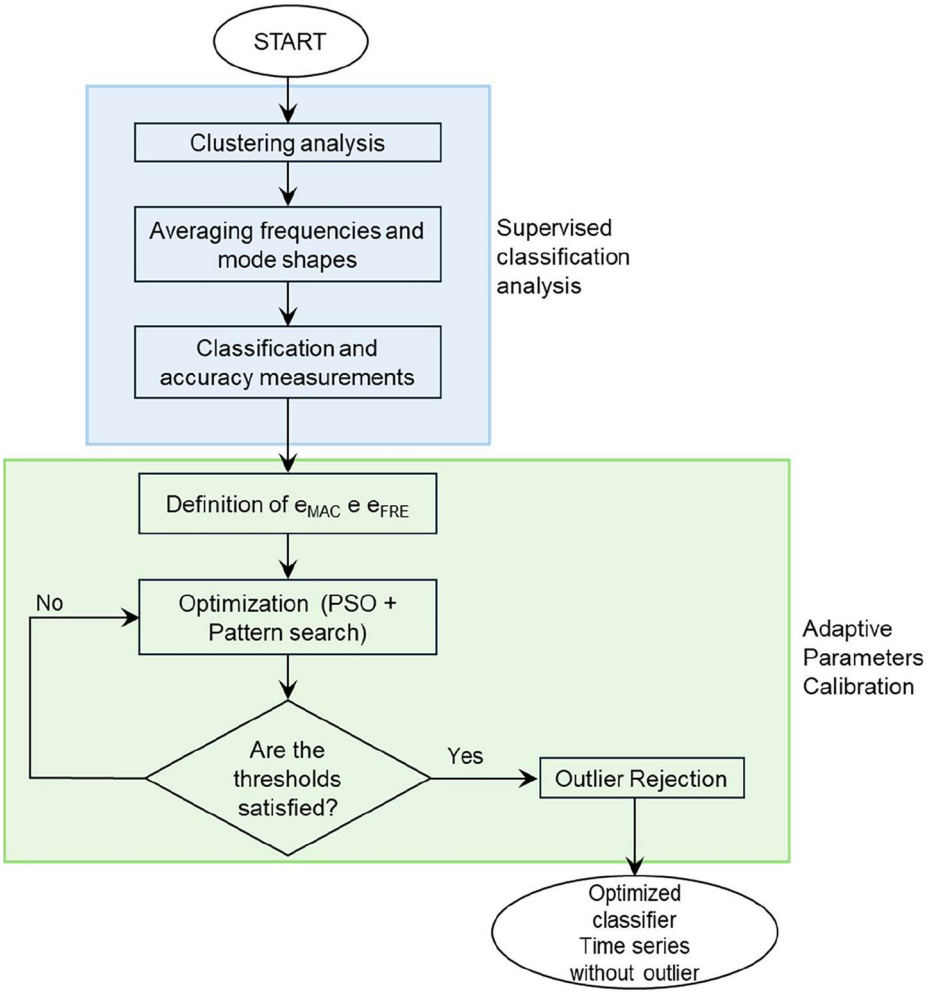


Fig. 1 Flowchart of the proposed method of Mode Tracking

as the difference in normalized frequency. These dual thresholds define a narrow acceptance window around each expected natural frequency, allowing the decision boundaries to be placed independently for each vibrational mode. Consequently, when two vibrational modes are closely spaced in frequency, one can position one acceptance interval between its neighbour values, separating the two classes in the feature space. Then, adopting an automated procedure each mode frequency distribution is modified; the algorithm models it as a two-component (bimodal) Gaussian (see Section 2.) and then adjusts the two weights of the bimodal model to eliminate any secondary peak. In practice, this means the cost function of an optimization is driven to collapse each natural frequency histogram to a single statistical mode (one dominant Gaussian peak). As a result, each tracked natural frequency time history converges to one continuous cluster of frequencies, ensuring that its identification remains statistically consistent over time. The Gaussian assumption is adopted for its gen-

erality and analytical convenience. In more detail, each mode natural frequency fluctuation around a mean value tends to be roughly symmetric due to the effects of EOVs and observation noise, while a mixture of two Gaussians provides a simple parametric form to detect and suppress any spurious secondary cluster.

The automatic procedure consists of a calibration of the threshold parameters for each vibration mode and the weighting factor between e_{MAC} and e_{freq}, based on an optimization algorithm. The goal of the optimization algorithm is to find the optimal parameter x, that represents a generic value of the thresholding quantities to be found for each mode class including the weighting factor that is the same for any mode class, based on a Particle Swarm Optimization (PSO) algorithm combined with a pattern search method (Torczon 1997). Specifically, during the optimization process, for each iteration i , the algorithm identifies a local minimum, x_i, corresponding to the value of the objective function J_i. The optimization algorithm has the following goals:

(I) Minimize the number of statistical modes (peak of Probability Density Function - PDF) in the distribution of values within a vibrational mode class, i.e. the most frequent value in a set of data into a class *k*.
(II) Minimize the number of missing values (i.e. unclassified data).

Regarding the first target, the algorithm is based on the concept that, within a class, during the optimization, the vibrational modes can be distributed according to a PDF having more statistical modes. This can happen for example when two vibrational modes are close in frequency values. In such a case, a bimodal distribution would represent the frequency domain, where each statistical mode would be associated to a specific undefined class of vibrational mode. However, if the thresholds e_{MAC} and e_{freq}(and their weighting factor) are chosen in an optimal way, the natural frequency distribution calculated over a class would converge to a single statistical mode distribution.

2.2.1 Cost function definition

The study proposal is founded on the principle that the thresholds e_{MAC} and e_{freq}, along with their associated weighting factor, can be systematically optimized to either maximize or minimize the proportion factor *p* within a generic bimodal distribution. In such a way, the bimodal distribution is adopted in the optimization process to ensure the assignment of a unique frequency value to each class. The resulting frequency histogram can be fitted to estimate the structural natural frequency PDF with a single statistical mode. This means that only one natural frequency will prevail over the others inside a mode class k_i. Due to its generality, the framework proposes the use of Gaussian distribution *g*, which can be adapted to fit a large class of statistical distributions, provided a reasonable boundary on the approximated random variable, e.g., natural frequency. The associated bimodal Gaussian (Reynolds 2009) PDF can be written as follows:

$$\begin{aligned} g\left(f|\mu_1,\sigma_1^2,\mu_2,\sigma_2^2\right) &= p\cdot g_1\left(f|\mu_1,\sigma_1^2\right)+(1-p)\cdot g_2\left(f|\mu_2,\sigma_2^2\right) \\ \mu &= \mathbb{E}\left[f\right] \\ \sigma^2 &= var\left[f\right] \end{aligned} \tag{4}$$

where g_1 and g_2 are the two components of the gaussian model, while the proportion factor p(i.e. the weighting parameter), is bounded between 0 and 1.

Since both minimizing and maximizing p lead to an equally valid result, i.e., obtaining a PDF with a single statistical mode, it is necessary to establish a strategy for selecting the optimization objective. To this end, it is first crucial to define a function that expresses the concept of class separation (Kotsiantis et al. 2007), based on the proportion p, during the optimization iterations. On the one hand, it is known that extreme values ($p=0$ or $p=1$) represent an optimal condition; on the other hand, a value of $p=0.5$ would indicate a class containing distinct values of natural frequency (two statistical distributions with the same weight). This suggests that the tracking of a specific mode follows a bifurcated trend over time, i.e. a clear symptom of a failed mode tracking process. Given these three boundary conditions for p, a relationship for y can be constructed. y is a function that serves as an error term in the objective function, ensuring that each class contains only natural frequencies belonging to a single statistical distribution, not necessarily Gaussian, corresponding to a single vibration mode information. Since a parabolic function can be defined through three points, and y represents an error term in the cost function, the following unique points can be assigned in the – plane: (0,0), (0.5,1), and (1,0), i.e.:

$$y = 4 \cdot \left(p - p^2\right) \tag{5}$$

The smaller the value of y, the more the single class of mode k will be characterized by a natural frequency history without bifurcation in time. Keeping only the term y in the cost function could lead to a trivial solution, where the optimal value of y is achieved for natural frequency time histories that correspond to empty classes. To prevent this, an additional component must be introduced to weigh the value of y based on the number of unclassified terms of the variable f across different classes. To this end, a term w, which represents the number of unclassified terms for a given reference mode to be tracked, normalized by the total number of initial elements belonging to a specific class, can be introduced. Both y and w take values between 0 and 1. The closer y is to zero, the more the frequency time history of a reference mode will be free from bifurcations. Similarly, the closer w is to zero, the denser the dataset will be. To ensure sensitivity to variations even when y or w assume intermediate values the authors propose to combine the error components in their geometric mean J_k for each class k:

$$J_k = \sqrt{w_k y_k} \tag{6}$$

This approach allows for detecting variations in the cost function,

$$J = \sum J_k / K \tag{7}$$

even in cases where either w or y remains relatively small to each other. Here, K represents the total number of classes or reference vibration modes. At this stage, the optimization process aims to determine the optimal thresholds e_{MAC} and e_{freq}(and their weighting factor) that minimize J. After completing the optimization procedure, the resulting time series may exhibit residual outliers. Therefore, an Outlier Rejection (OR) process is suggested (Tallón-Ballesteros and Riquelme 2014; Sharma et al. 2015), which involves fine-tuning the

thresholding parameters based on the values identified by the MT algorithm. This step is preparatory for the use of vibration frequency time histories, which can be then employed as training and validation datasets for machine learning classifiers.

3 Validation with numerical benchmark

To verify the effectiveness of the above-proposed MT method, it was applied to a reference MDoF chain-like system. Indeed, an application of this type represents the simplest system in which the MT problem can arise. The reference system is characterized by 7 DoF, a Damping ratio (ζ) of 4%, a density (ρ) of 1200 kg/m², and a first natural frequency (f_1) of approximately 3.05 Hz.

Four testing systems, simulating various types of real buildings, were derived from the reference model by introducing perturbations in its modal properties. These perturbations were applied using different PDFs. Each of these testing systems was characterized by a distinct statistical distribution of the natural frequency, assumed to be known. However, it appears clear that the PDFs of real systems remain unknown, as they can only be determined after the mode tracking process. By applying the proposed method to the four testing systems, a direct comparison between the PDF estimated after the MT procedure and the actual PDF allows for an assessment of the error associated with the proposed method. It is important to underline that, although a bimodal Gaussian distribution is assumed for class separation, it does not necessarily represent the actual distribution that the natural frequencies will follow after MT. The Gaussian assumption is, in fact, applied solely for the purpose of class separation. Once this step is completed, the inference of the true distribution can be performed using appropriate techniques, which fall beyond the scope of this paper. In this study, the distribution estimation following the MT procedure is performed using Kernel Density Estimation (KDE) (Botev et al. 2010). The four testing systems are associated to the following statistical distributions: Normal (Forbes et al., (2011)c), Logistic (Forbes et al., (2011)a), Lognormal (Forbes et al., (2011)b), and Weibull (Forbes et al., (2011)d). To compare the values of natural frequencies tracked by the MT proposed method with the reference one, both the time series and the PDFs of natural frequencies were overlaid. The reference testing systems represent the *ground true,* as they provide the real PDF (which is typically unknown in real case studies) that should be obtained after the MT procedure. Figure 2 contains superimposed time series and the corresponding PDFs for the first natural frequencies of the four different testing systems. Specifically, it presents the comparison between:

- The time series of frequencies of the MDoF system exhibiting behavior consistent with a Normal distribution and the values estimated by the proposed MT method (Fig. 2 (a));
- The PDF of the Normal distribution and the PDF obtained through kernel fitting applied to the values estimated by the MT process (Fig. 2 (b));
- The time series of frequencies of the MDoF system exhibiting behavior consistent with a Logistic distribution and the values estimated by the MT method (Fig. 2 (c));
- The PDF of the Logistic distribution and the PDF obtained via kernel fitting on the MT-estimated values (Fig. 2 (d));
- The time series of frequencies of the MDoF system following a Lognormal distribution

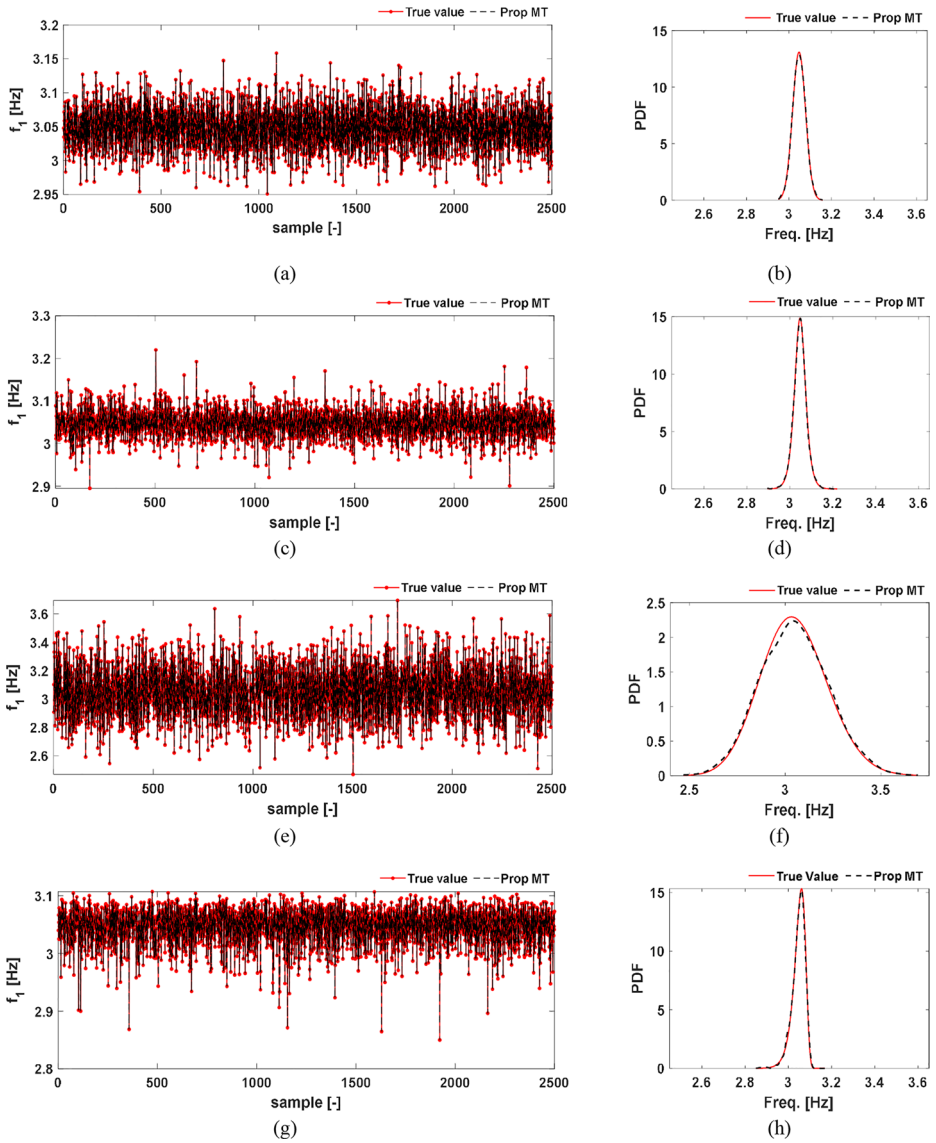


Fig. 2 Superimposed time series and the corresponding PDFs for the first natural frequencies of the four testing systems following different behaviour distributions

and the values estimated by the MT method (Fig. 2 (e));

- The PDF of the Lognormal distribution and the PDF obtained through kernel fitting on the MT-estimated values (Fig. 2 (f));
- The time series of frequencies of the MDoF system following a Weibull distribution and the values estimated by the MT method (Fig. 2 (g));
- The PDF of the Weibull distribution and the PDF obtained via kernel fitting on the MT-estimated values (Fig. 2 (h)).

This figure serves to illustrate the effectiveness of the MT method in accurately estimating frequency distributions for MDoF systems with varying statistical behaviours, providing insights into the consistency of the proposed method.

Some indicators were calculated to provide a measure of the accuracy of the proposed MT method. The following indicators were considered:

- Average value of the autocorrelation coefficient ($\mathrm{R_{avg}}$) (Ezekiel 1930);
- Deviation from the mean value ($\mathrm{D_{avg}}$), i.e., the average distance of the time series from their mean value;
- Number of unclassified data (ξ).

The following tables show the value of these indicators estimated by the MT procedure for each assumed testing system with the different distributions, compared to the true values supposed to be known in this validation numerical framework.

An additional parameter is introduced to provide a comparison between the PDFs of the testing systems and the distribution obtained via the MT proposed method. For this purpose, the Kullback–Leibler Divergence (D_{KL}) (Kullback 1951; Belov and Armstrong 2011) is considered, which represents the statistical distance between two distributions and is defined as:

$$D_{KL}(P||Q) = \sum P(x) \, log \frac{P(x)}{Q(x)} \tag{8}$$

where $P(x)$ denotes the PDF of the reference distributions (P_{ref}), (i.e. the normal, logistic, lognormal, and Weibull distribution), while $Q(x)$ represents the PDF of the values tracked using the proposed MT method (P_{MT}). Thus, in the present work, the previous equation becomes:

$$D_{KL}(P_{ref}||P_{MT}) = \sum P_{ref} log \frac{P_{ref}}{P_{MT}} \tag{9}$$

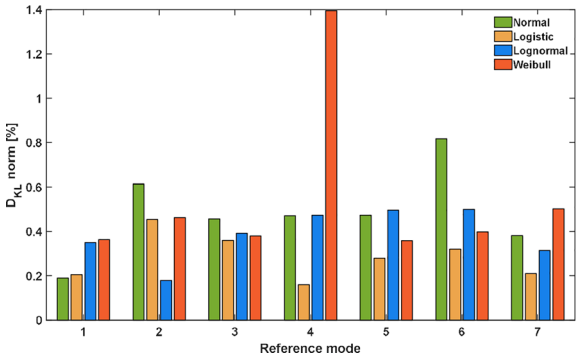
To obtain a reference-based value of D_{KL} and constrain this value between 0 and 1, a normalized value ($\hat{D}_{KL}$) was calculated using the PDF of the uniform distribution (P_{unif}) as reference. Specifically, the following quantity was determined:

$$\hat{D}_{KL} = \frac{D_{KL}}{D_{KL}^{max}} \tag{10}$$

where:

- D_{KL} is $D_{KL}(P_{ref}||P_{MT})$ as Eq. 9;
- D_{KL}^{max} is the D_{KL} between the PDF of a uniform distribution (P_{unif}) and the PDF of the reference distribution P_{ref}, so it is computed as:

$$D_{KL}^{max} = \sum P_{ref} log \frac{P_{ref}}{P_{unif}} \tag{11}$$



Mode	$\widehat{D}_{KL}$ [%]			
	Norm	**Logis**	**Lognorm**	**Weib**
1	0.1899	0.2050	0.3499	0.3631
2	0.6136	0.4541	0.1787	0.4629
3	0.4571	0.3595	0.3919	0.3803
4	0.4716	0.1594	0.4733	1.3954
5	0.4738	0.2790	0.4966	0.3591
6	0.8168	0.3208	0.5002	0.3979
7	0.3810	0.2104	0.3141	0.5017

Fig. 3 Bar plot showing the variation of normalized Kullback-Leibler Divergence ($\hat{D}_{KL}$) between the reference distributions considered and the distribution obtained using the proposed MT method

Table 1 Comparison between the true value of the *Normal* distribution and the data distribution obtained from the MT proposed algorithm: Autocorrelation (R_{avg}), Deviation from the average (D_{avg}), and the number of unclassified data (ξ)

Mode	R_{avg} %		D_{avg}		ξ %	
	True value	*MT*	*True value*	*MT*	*True value*	*MT*
1	3.97	3.97	0	0	0	0
2	4.86	4.88	0	0	0	0.12
3	4.34	4.34	0	0	0	0
4	4.76	4.76	0	0	0	0
5	5.16	5.16	0	0	0	0
6	4.35	4.35	0	0	0	0
7	4.93	4.93	0	0	0	0

Table 2 Comparison between the true value of the *Logistic* distribution and the data distribution obtained from the MT proposed algorithm: Autocorrelation (R_{avg}), Deviation from the average (D_{avg}), and the number of unclassified data (ξ)

Mode	R_{avg} %		D_{avg} %		ξ %	
	True value	*MT*	*True value*	*MT*	*True value*	*MT*
1	4.35	4.35	0	0	0	0
2	4.67	4.68	0	0	0	0.12
3	4.36	4.36	0	0	0	0
4	4.98	4.98	0	0	0	0
5	4.33	4.33	0	0	0	0
6	5.04	5.03	0	0.0007	0	0
7	4.28	4.28	0	0	0	0.04

Figure 3 represents a bar plot and a table with the values $\hat{D}_{KL}$ referenced to the PDF of each considered distribution and the PDF of the values obtained by the proposed MT method.

The data reported in (Tables 1, 2, 3 and 4) shows that the values of indicators are similar to each other. A slight variation in D_{avg} is observed in the case of the proposed MT method and, in the case of 2nd and 7th modes, the MT method registers a very limited number of unclassified data. Regarding the R_{avg} values, they remain nearly unchanged. These findings

Table 3 Comparison between the true value of the the *Lognormal* distribution and the data distribution obtained from the MT proposed algorithm: Autocorrelation (R_{avg}), Deviation from the average (D_{avg}), and the number of unclassified data (ξ)

Mode	R_{avg} %		D_{avg} %		ξ %	
	True value	*MT*	*True value*	*MT*	*True value*	*MT*
1	4.87	4.87	0	0	0	0
2	4.40	4.42	0	0	0	0.12
3	4.22	4.22	0	0	0	0
4	4.49	4.49	0	0	0	0
5	4.86	4.86	0	0	0	0
6	4.58	4.53	0	0.0019	0	0
7	4.53	4.52	0	0.0014	0	0.04

Table 4 Comparison between the true value of the *Weibull* distribution and the data distribution obtained from the MT proposed algorithm: Autocorrelation (R_{avg}), Deviation from the average (D_{avg}), and the number of unclassified data (ξ)

Mode	R_{avg} %		D_{avg} %		ξ %	
	True value	*MT*	*True value*	*MT*	*True value*	*MT*
1	4.16	4.16	0	0	0	0
2	4.90	4.90	0	0	0	0.12
3	4.35	4.35	0	0	0	0
4	4.57	4.57	0	0	0	0
5	5.28	5.28	0	0	0	0
6	4.88	4.89	0	0.0005	0	0
7	4.54	4.55	0	0	0	0.04

are further corroborated by the $\hat{D}_{KL}$ values (Fig. 3), where the difference values fall within the range of 0.1% to 0.9%, except in the case of the Weibull distribution for the 4th mode, where a greater discrepancy is noted between the values of the reference distribution and those tracked by the proposed MT method. However, although higher, the value reached is 1.4%, which is still very small.

4 Application on a full-scale structure

4.1 Case study description

The Church of Santa Caterina (Fig. 4) in Casale Monferrato, built in the first half of the 18th century, is one of the most significant examples of the Baroque in Piedmont and certainly the most important of the 18th century sacred architecture of Casale Monferrato. It was built by Giacomo Zanetti, based on the project by Giovanni Battista Scapitta, between 1718 and 1726. The church is part of the architectural ensemble that includes the church itself and the choir attached to it in the part behind the presbytery (Fig. 5). The structure has a Greek cross plan, and the central hall is covered by an elliptical dome set on an eight-segment windowed drum. Above the dome, a lantern was created with eight windows surmounted by an elliptical dome. The main façade, facing Piazza Castello, has an overall vertical development of approximately 19 metres, however, starting from the level of the drum shutter, which is



Fig. 4 The Church of Santa Caterina: (**a**) Façade of the Church from Piazza Castello; (**b**) lantern of the Church and (**c**) internal view of the Church

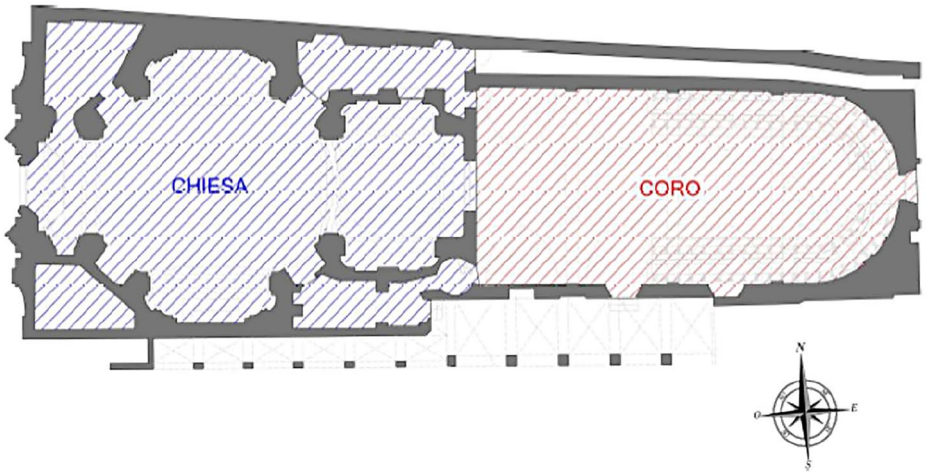


Fig. 5 Plan of the Church of Santa Caterina

located at 13 m, the façade continues cantilevered into the tympanum for approximately 6 metres. The drum is located at a height of 13 meters and rises approximately 7 metres; it has an elliptical plan whose major axis is approximately 14 meters long and the minor one approximately 10 meters. The external surface is marked by eight pilasters supporting the dome-lantern system. The oval-shaped dome is placed on the drum and is approximately 5 meters tall. There are eight ribs that connect to the drum pilasters, the ribs are interspersed with masonry levels. The dome is covered with a thin layer of copper plates directly fixed to the external masonry. In Fig. 6, the geometrical survey of the church is reported.

The Church was interested by a una-tantum monitoring campaign during 2010; this allowed to obtain the fundamental dynamic parameters of the structure. More recently, a

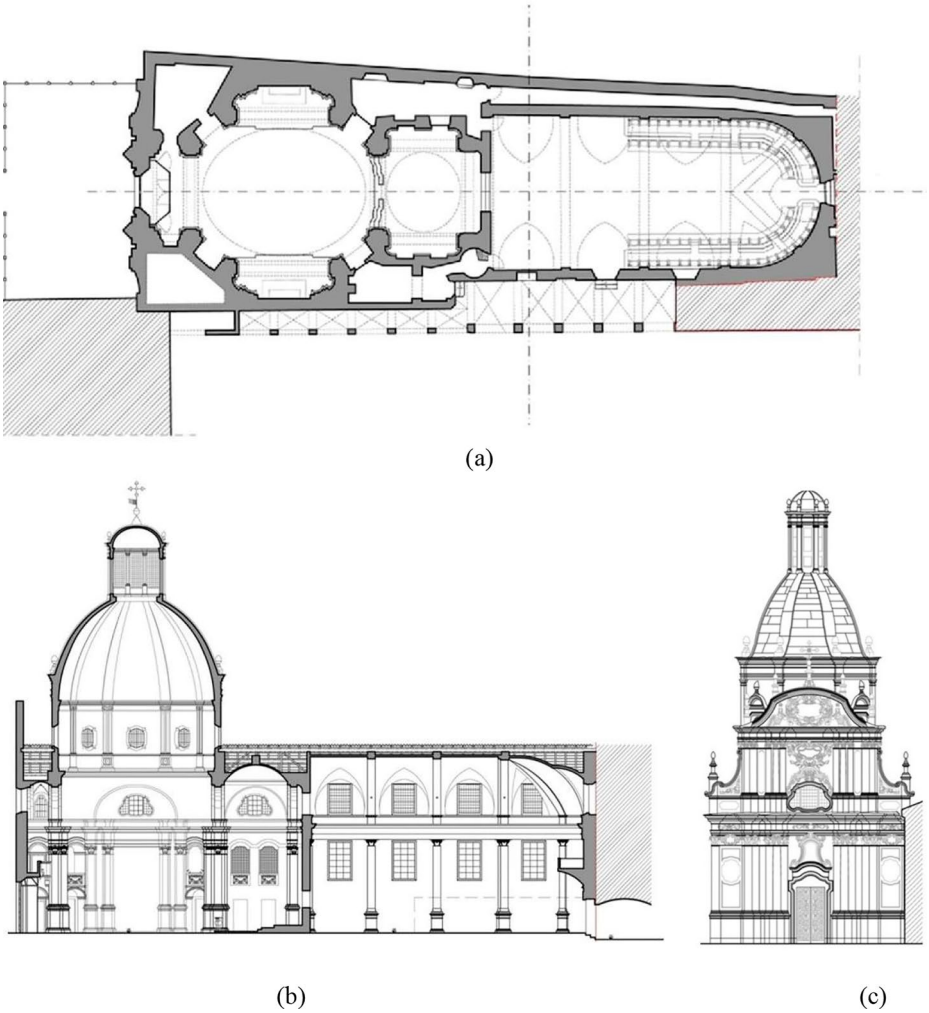
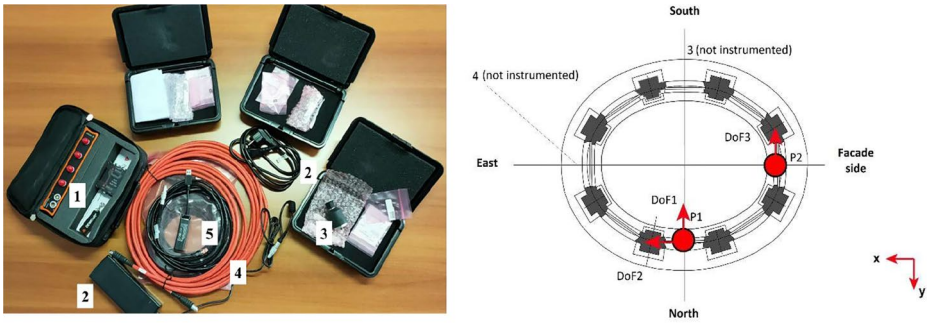


Fig. 6 Drawings from the geometrical survey of the church of Santa Caterina: (**a**) in-plan view, (**b**) longitudinal section, (**c**) front view from Piazza Castello

new long-term monitoring campaign was performed between December 2022 and March 2023. In detail, this latest campaign was divided into two periods: the first between December and January (22.12.2022–09.01.2023) and the second between February and March (21.02.2023–17.03.2023). The experimental tests were done in ambient vibration in order to extract the structural modal parameters through OMA techniques. Moreover, these experimental tests allowed to track the evolution of the natural frequencies in time. The experimental setup of the monitoring system was characterized by three dynamic sensors, i.e. accelerometers (high sensitivity seismic accelerometer, ceramic shear ICP® 393B12 model, 10 V/g, 0.15 to 1k Hz, 2-pin top connection) located on top of the lantern in order to catch the diaphragmatic vibrations of this structural component. The accelerometers have been installed as follows:



(a) (b)

Fig. 7 (**a**) Acquisition system and accelerometers of the monitoring system and (**b**) layout of the experimental setup

Table 5 Channel data of the experimental setup

Degre of Freedom	*Data*	*Channel*	*Sensor*	*Position*	*Direction*	*Name*	*Sign*
1	Accel	2	2	1	Y	1Y	−1
2	Accel	3	3	1	X	1X	1
3	Accel	4	4	2	Y	2Y	−1

- Two accelerometers to record the accelerations in the transversal direction;
- One accelerometer to record the acceleration in the longitudinal direction of the lantern.

In Fig. 7 the acquisition system and the layout of the experimental setup of the Church of Santa Caterina are shown, while in Table 5 the setup is described. In detail, the monitoring system consists of:

1. One dynamic four-channel Dewesoft® acquisitor (i.e., KRYPTON-4xACC, 4 channel single ended Krypton slice for Voltage, IEPE).
2. Electric cables to supply power to the acquisitor.
3. Accelerometers with cables that allow the analog signal (Volt) to reach the acquisitor.
4. Cable where digital information travels from the acquisitor towards data exchange control unit.
5. Cable where digital information travels from a data exchange control unit towards a computer.

During the acquisition procedure, the recorded signals were sent to a workstation located in the Earthquake Engineering and Dynamics laboratory (EED lab) of the Politecnico di Torino and stored there. Then, the signals were pre-processed and then used to identify the natural frequency of the structure.

4.2 Application of the proposed method

Once the data has been acquired and preprocessed, the SSI identification (Overschee and Moor 1996) algorithm was used to obtain the natural frequencies of the structure. Then,

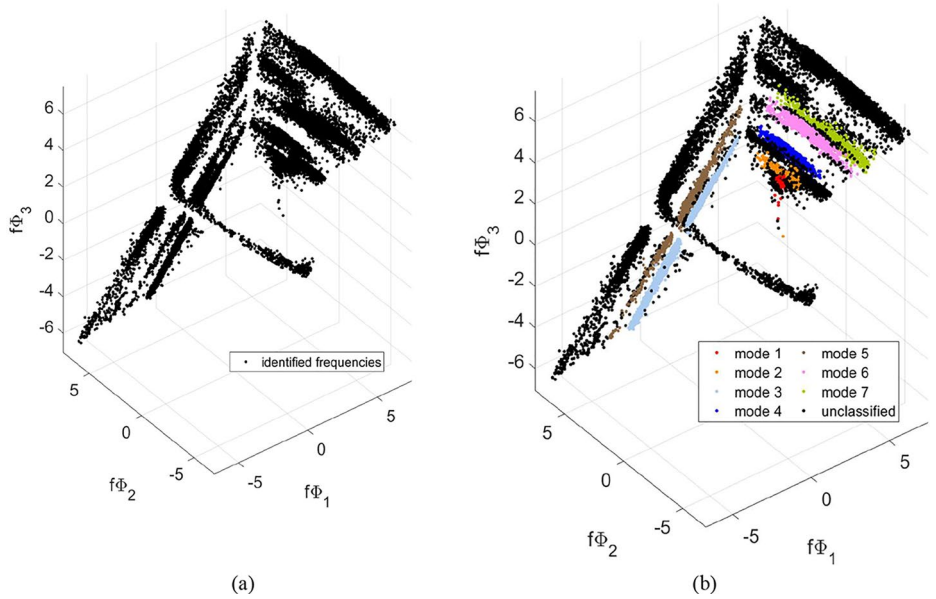


Fig. 8 (**a**) Identified mode shapes scaled relative to the associated frequency. (**b**) Manual cluster: each coloured cloud represents a different identified mode (i.e., red – mode 5, orange – mode 6, light blue – mode 7, blue – mode 8, brown – mode 9, pink – mode 10, and green – mode 11)

Table 6 The set of assumed reference modes

Identifier	*Description*	f_n*[Hz]*
1	Lantern moves transversally.	3.05
2	Lantern moves mainly transversally with little longitudinal effects.	3.45
3	Lantern moves mainly longitudinal with little transverse effects.	3.88
4	Lantern moves mainly transversally with lower components in longitudinal direction.	4.06
5	Lantern moves mainly longitudinally with lower components in transverse direction.	4.49
6	Lantern moves transversally, and very little in the longitudinal direction.	5.19
7	Local torsion mode of the lantern.	5.51

through preliminary clustering, the selection of natural frequencies of the Church of Santa Caterina is developed from all those identified with the SSI algorithm. All the identified mode shapes are normalized to their maximum value, then they are pre-multiplied for the corresponding natural frequencies and plotted in a 3D plane (Fig. 8 (a)). This representation unveils the longitudinal and/or transversal nature of each mode shape, since it is known that the coordinates of the eigenvectors, $\phi_{k,i}$(with i=1,2,3) are: (i) $\phi_{k,1} = \phi_{k,y1}$ derived from the accelerometer in Y direction, (ii) $\phi_{k,2} = \phi_{k,x1}$ from the accelerometer in X direction, and (iii) $\phi_{k,3} = \phi_{k,y2}$ from the second accelerometer in Y direction. By cross-referencing the information from the latter representation and those from the previous preliminary experimental campaign of 2010 (Table 6) the main modes are clustered in a sub domain

of engineering interest (0.5–7 Hz). As reported in Table 6, seven modes are expected to be found in the *scaled mode shapes space*, and, exploiting the descriptions, the main direction of motion for each mode is highlighted. Thus, in the *scaled mode shapes space*, the point cloud for each mode is selected by clustering the points closed to the reference natural frequency value and in the main direction of motion reported in Table 6.

The clustering results are presented in Fig. 8 (b), where the black points represent the rejected modes, as they fall outside the context of engineering interest. To clean the selected values of each mode from disturbances and slight variances, an *average procedure* was followed. Since the acquired signals are 20 minutes long, pairs of consecutive signals (i.e., 10 + 10 minutes in duration) were considered, from which at most one frequency value and one mode shape for each class of modes is obtained by averaging the values of the two considered signals. In this way, for each acquisition, one frequency value and one mode shape were obtained. The results from this clustering analysis are then used as input for an adaptive parameter calibration, with the ultimate goal of excluding outliers and defining the time histories of the natural frequencies of the church. A preliminary SVM model has been trained and applied to classify the identified structural modal quantities, with the goal of obtaining the reference mode set as the mean value of each cluster.

Once the results of the classification analysis were obtained, they were used to perform the MT proposed method. From the results of the initial analysis, the time histories obtained are characterized by various values that deviate significantly from the average natural frequency values and can therefore be identified as outliers. For this reason, the authors applied an Outlier Rejection (OR) process capable of filtering these values from the time histories, based on the concept of *MAC* and frequency deviation. The OR procedure was carried out by fine tuning the thresholds for the MAC discrepancy ($MAC_{thr} = 1 - e_{MAC}$) and the frequency discrepancy (e_{freq}). This fine tuning of the threshold values was performed starting from the observation of the obtained time-histories of the variables MAC_{thr} and e_{freq}, calculated starting from the results of the MT. In this way, it was possible to define the following values of thresholds (Table 7).

Once the previous threshold values were defined, they were provided to the optimization algorithm to lead it in finding the optimal values to track the modal characteristics. Therefore, the analysis was repeated with these values and the time series of the natural frequencies were found (Fig. 9), in this case cleaned of almost all the outliers, and ready to be passed for training the final SVM classifier.

Table 7 Thresholds for the MAC (MAC_{thr}) and the frequency (e_{freq}) used in the fine tuning process for the OR

Mode	*Thresholds*	
	MAC_{thr}	e_{freq}
1	0.9985	0.02875
2	0.9923	0.04115
3	0.9835	0.04181
4	0.9774	0.03214
5	0.9818	0.03707
6	0.9854	0.02912
7	0.9917	0.02585

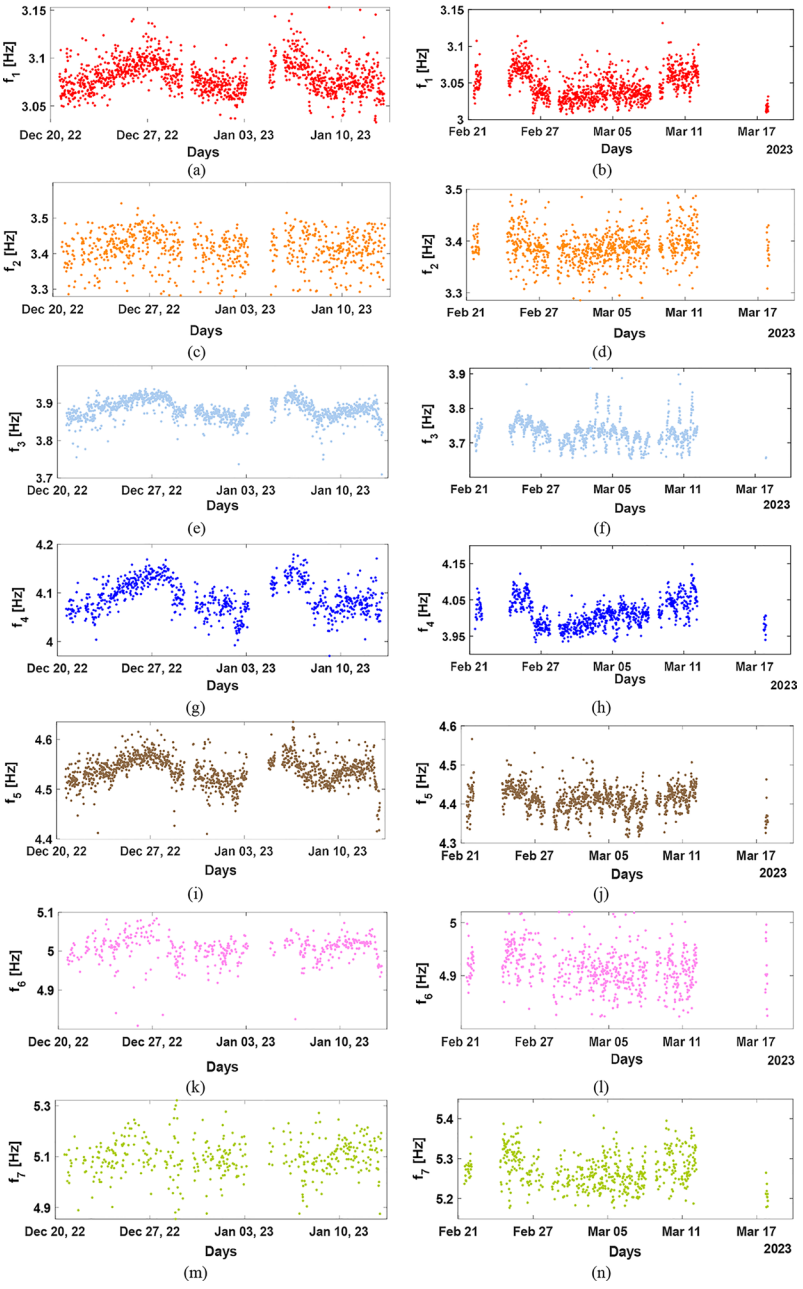


Fig. 9 Results of proposed MT algorithm after OR process: (**a**) 1st frequency in the 1st considered period, (**b**) 1st frequency in the 2nd considered period, (**c**) 2nd frequency in the 1st considered period, (**d**) 2nd frequency in the 2nd considered period, (**e**) 3rd frequency in the 1st considered period, (**f**) 3rd frequency in the 2nd considered period, (**g**) 4th frequency in the 1st considered period, (**h**) 4th frequency in the 2nd considered period, (**i**) 5th frequency in the 1st considered period, (**j**) 5th frequency in the 2nd considered period, (**k**) 6th frequency in the 1st considered period, (**l**) 6th frequency in the 2nd considered period, (**m**) 7th frequency in the 1st considered period, and (**n**) 7th frequency in the 2nd considered period

4.3 Comparison between FFD algorithm and proposed MT method

Before defining the classifier using the new filtered values, the authors decided to test the effectiveness of the proposed method by comparing it with another widely used approach in the literature for MT. The other considered method is the FDD method (Brincker et al. 2001), which was previously mentioned in the introduction, along with a discussion of its limitations. This algorithm was applied to the real case study, and the results obtained are shown in Fig. 10. In particular, only modes 1st, 6th, and 7th are shown for brevity. By analyzing the value of ξ, it can be observed that for the 2nd mode, 76% of the data is missing, while for modes 3rd, 4th and 5th, more than 99% of the data is missing. The values for D_{avg} and R_{avg} do not show significant differences. However, it is important to consider these indicators in a relative perspective rather than an absolute one. In other words, the values of D_{avg} and R_{avg} should be interpreted in relation to the value of ξ. Since these indicators are calculated based on time histories composed of very few data points, the resulting values are unreliable. In the case of the 6th mode, the highest D_{avg} value was observed; however, it is reported because FDD was still able to track the trend of the time series in a reasonable manner, albeit with slightly higher values. The comparison between the two methods shows that, in situations such as the one treated here, involving a sparse sensor configuration and a complex structure as a church, the FDD algorithm has difficulty tracking the modes accurately. It remains applicable for the first mode, where it produces acceptable results with

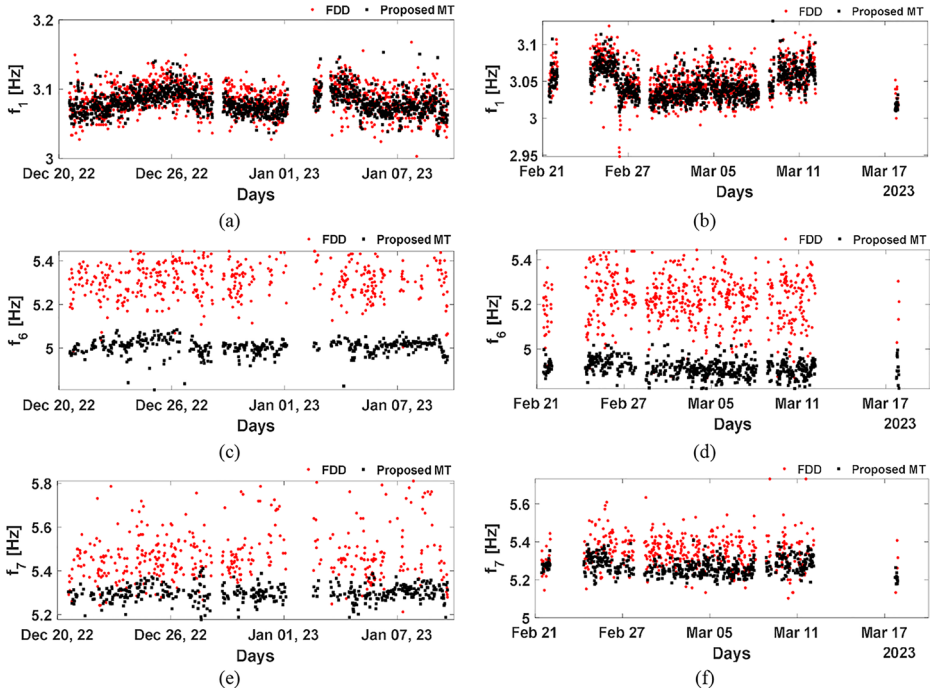


Fig. 10 Comparison of frequency time series obtained through the FDD method and the proposed MT approach: (**a**) 1st frequency in the 1st considered period, (**b**) 1st frequency in the 2nd considered period, (**c**) 6th frequency in the 1st considered period, (**d**) 6th frequency in the 2nd considered period, (**e**) 7th frequency in the 1st considered period, and (**f**) 7th frequency in the 2nd considered period

minimal deviation. However, as the analysis progresses, FDD fails to capture the higher modes, as already shown in (González and Boroschek 2020). The main advantage of FDD is that it is less time-consuming; however, it becomes inapplicable due to the previously mentioned aspects.

In Table 8 the results in terms of R_{avg}, D_{avg}, and ξ are reported. It can be noticed that the proposed method generally outperform the FDD based MT algorithm, producing time series that are characterized by an higher autocorrelation (about two times), a lower dispersion from the average value (56% less), and a lower percentage of unclassified data ξ (27% respect to about 70%).

4.4 Definition of final classifier

At the end, the corrected time-series, so those obtained after the OR process, were used to train the final SVM model. The SVM model is trained and validated on a dataset containing 45,828 3-dimensional features $f_k\mathbf{\Phi}_k = [f_k\phi_{k,1},\ f_k\phi_{k,2}, f_k\phi_{k,3}]$. The labels assigned for the supervised binary classification are related to the structural modes and rejected modes (1 and 0). The aim of this model is to classify the structural identified mode correctly and automatically. The training dataset represents the 75% of the entire data available (Fig. 11) and during the training process, a five-fold cross validation is conducted. The remaining 25% is considered for testing purposes. The optimized hyperparameters are shown in Table 9. The model validation gives an accuracy of 99.7%. The validation confusion matrix is shown in Fig. 12, while the remaining 25% of data related to the testing dataset is tested on the model, giving an accuracy of 99.7% (Fig. 11 (b)). The testing confusion matrix is represented in Fig. 12.

After removing the rejected modes from the original dataset, a second model has been developed for structural modal classification with 8887 3-dimensional features. Labels are assigned to the different identified modes (1–7). This second model relies on a linear SVM. Here, same consideration for dataset partition as the first model has been made (training dataset 75%, testing dataset 25%). In Fig. 13(a), the training dataset, with the corresponding assigned labels is shown. The accuracy related to the model validation is 100%, same result for the testing, leading to a perfect multiclass classification. In Fig. 13(b), the predicted testing features and labels are reported, while the validation confusion matrix and the testing confusion matrix are shown in Fig. 14. The final SVM model can be thus used for MT of new available data.

Table 8 Comparison of FDD method and the MT proposed algorithm: Autocorrelation (R_{avg}), Deviation from the average (D_{avg}), and the number of unclassified data (ξ)

Mode	R_{avg} %		D_{avg} %		ξ %	
	FDD	*MT*	*FDD*	*MT*	*FDD*	*MT*
1	55.59	70.97	0.78	0.67	2.27	0.47
2	21.60	20.11	3.48	0.95	76.81	30.99
3	44.78	90.09	2.01	2.02	98.24	7.84
4	9.47	83.23	1.97	1.11	99.10	31.80
5	30.25	87.41	1.03	1.42	99.31	7.42
6	25.18	63.81	6.09	1.00	55.81	54.14
7	34.14	28.55	2.48	0.65	61.64	59.45
Average	31.57	63.45	2.55	1.12	70.45	27.44

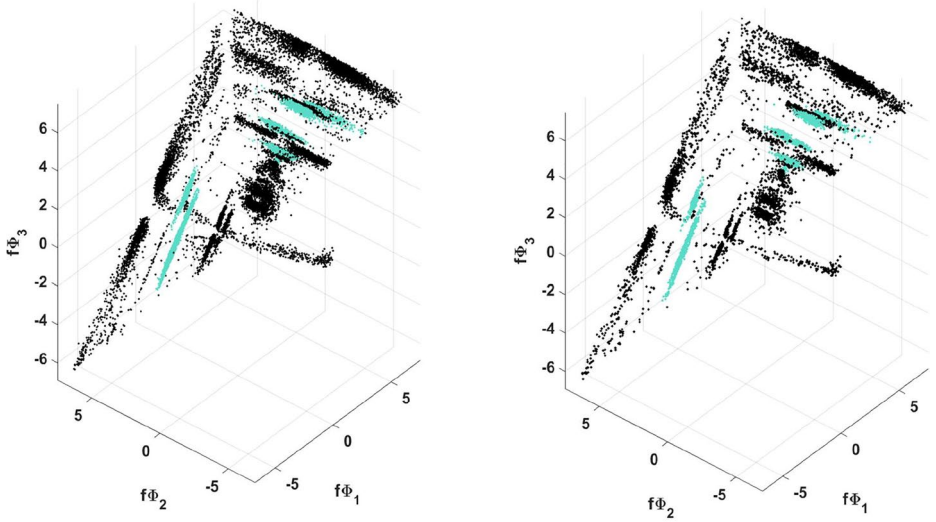


Fig. 11 (**a**) Training dataset for the optimizable SVM model. In black the outliers are shown, while the green label is attributed to the structural modes. (**b**) Testing dataset for the optimizable SVM model. In black the predicted outliers are shown, while the green label is predicted and attributed to the structural modes

Table 9 SVM optimizable hyperparameters

Hyperparameter	*value*
Multiclass method	One-vs-All
Box constraint level	171.34
Kernel scale	0.25
Kernel function	Gaussian
Standardized data	false

5 Conclusions

This paper presents a novel automatic MT procedure designed to estimate the time series of natural frequencies from long-term seismic monitoring systems. MT process is essential for monitoring the structural health of buildings and infrastructure. However, traditional methods exhibit several limitations: they require manual intervention, struggle to distinguish closely spaced frequencies, and often fail to ensure consistent classification, particularly in the case of highly complex structures and sparse sensor configurations. The proposed method addresses these challenges through an automatic optimization process based on PSO combined with a pattern search approach allowing for the automatic tracking of the natural frequency time histories of the structure. This methodology precisely adjusts the threshold parameters and weighting factors between frequency and MAC residuals, ensuring a more accurate classification of vibrational modes. A key innovation of the proposed approach is the incorporation of a cost function designed to reduce the occurrence of multiple statistical modes within a vibrational class while simultaneously minimizing unclassified data. By modeling the frequency distribution using a bimodal Gaussian function, the

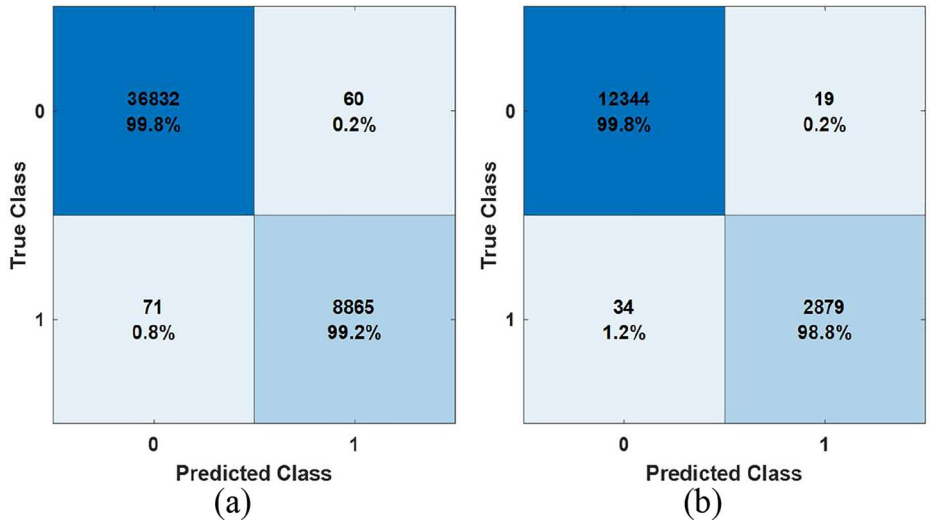


Fig. 12 (**a**) Validation Confusion Matrix for the optimizable SVM (top: number of observations; bottom: percentage rates). The label 0 represents the outlier class; the label 1 represents the structural modes class. (**b**) Testing Confusion Matrix for the optimizable SVM (top: number of observations; bottom: percentage rates). The label 0 represents the outlier class; the label 1 represents the structural modes class

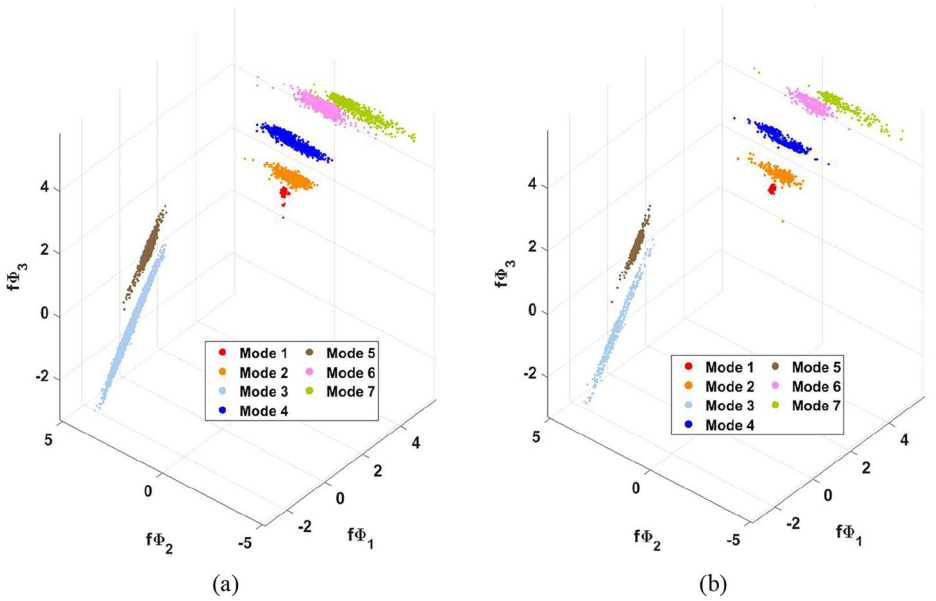


Fig. 13 (**a**) Training dataset for the linear SVM model. The labels attributed to the structural modes are coloured in a different way (i.e., red – mode 5, orange – mode 6, light blue – mode 7, blue – mode 8, brown – mode 9, pink – mode 10, and green – mode 11). (**b**) Testing dataset for the linear SVM model. The labels predicted and attributed to the structural modes are coloured in a different way (i.e., red – mode 5, orange – mode 6, light blue – mode 7, blue – mode 8, brown – mode 9, pink – mode 10, and green – mode 11)

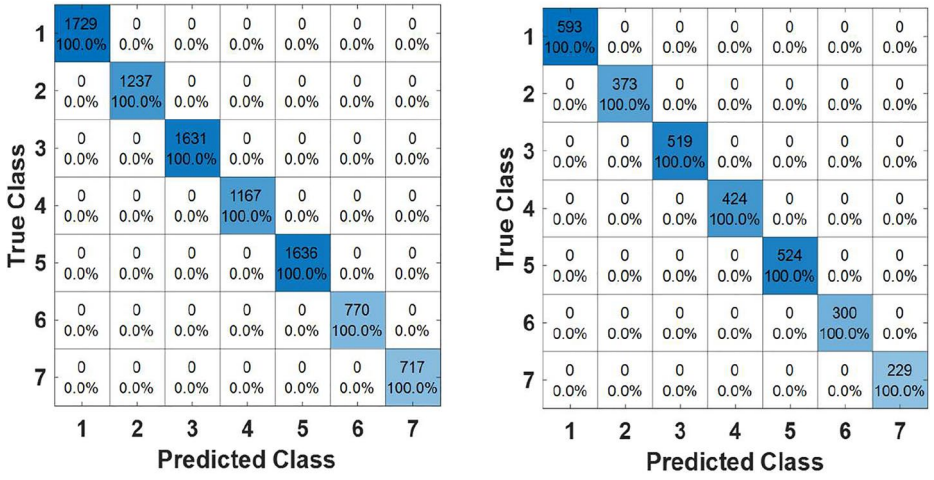


Fig. 14 (**a**) Validation Confusion Matrix for the linear SVM (top: number of observations; bottom: percentage rates). The label 5 represents Mode 5, etc. (**b**) Testing Confusion Matrix for the linear SVM (top: number of observations; bottom: percentage rates). The label 5 represents Mode 5, etc

method ensures that each mode class converges towards a single dominant frequency. The optimization strategy seeks to minimize an error that tracks bifurcations in mode identification, ensuring stable classification over time. Furthermore, an OR process is introduced to refine the results, making the method particularly suitable for generating clean datasets for machine learning classifiers. Compared to existing techniques, this approach offers a higher level of accuracy in MT when a limited number of sensors is available.

The method was first verified numerically on a MDoF chain-like system and then tested on a complex monumental building, the Church of Santa Caterina in Casale Monferrato. Given the structural complexity of this monumental building, the limited number of sensors available, and the characteristics of its structural modes, conventional MT methods, such as manual tracking or FDD, were deemed unfeasible. Based on the results presented in this paper, the proposed MT algorithm demonstrates improvements over the traditional FDD methods, which are outlined hereinafter:

- The proposed MT algorithm yields higher autocorrelation values, approximately twice those of the FDD method. This indicates that the MT algorithm provides more coherent modes over time, leading to enhanced tracking of vibrational modes.
- The proposed MT method exhibits a lower variance of natural frequency from the average compared to FDD, showing a reduction of about 56%. This suggests that the MT algorithm produces more accurate results.
- The proposed MT approach significantly reduces the amount of unclassified data, with only 27% remaining unclassified compared to the 70% observed with FDD.

To further validate the effectiveness of the presented method, it could be extended to other historical structures, such as bell towers, or to different typologies of structures, including

bridges and viaducts, with different sensor configurations and different structural features. This would also help to overcome the intrinsic limitations of the proposed procedure, the main one being the need to customize and calibrate it for use in each specific structural context. Furthermore, further insights concern the statistical assumptions on which the methodology is based, which will be the subject of future numerical and experimental applications.

Acknowledgments This publication is part of the project PNRR-NGEU, which has received funding from the MUR-DM 118/2023. Experimental tests were conducted within the activities of Camelot PoC Instrument Project. The authors gratefully acknowledge the Collegio Convitto Municipale Trevisio di Casale Monferrato, the Santa Caterina Onlus and its president Marina Buzzi Pogliano, Arch. Enrica Caire, Eng. Simone Giordano, Arch. Sara Vecchiato.

Author contributions Conceptualization S.C., G.M and R.C; Methodology C.S. and G.M.; Validation S.C. and G.M.; Formal analysis S.C., G.M., A.C. and V.C.; Investigation S.C., G.M., A.C. and V.C.; Resources S.C. and G.M.,; Data curation S.C., G.M., A.C. and V.C.; Writing—original draft preparation S.C., G.M., A.C. and V.C.; Writing—review and editing S.C., G.M. and R.C.; Visualization S.C., G.M. and R.C.; Supervision R.C.; Project administration, R.C.; Funding acquisition, R.C

Funding The authors declare that no funds, grants, or other support were received during the preparation of this manuscript.

Data availability Data employed in the current study are available from the corresponding author on reasonable request.

Declarations

Conflicts of interest The authors declare that they have no known competing financial interests or personal relationships that could have appeared to influence the work reported in this paper.

Open Access This article is licensed under a Creative Commons Attribution-NonCommercial-NoDerivatives 4.0 International License, which permits any non-commercial use, sharing, distribution and reproduction in any medium or format, as long as you give appropriate credit to the original author(s) and the source, provide a link to the Creative Commons licence, and indicate if you modified the licensed material. You do not have permission under this licence to share adapted material derived from this article or parts of it. The images or other third party material in this article are included in the article's Creative Commons licence, unless indicated otherwise in a credit line to the material. If material is not included in the article's Creative Commons licence and your intended use is not permitted by statutory regulation or exceeds the permitted use, you will need to obtain permission directly from the copyright holder. To view a copy of this licence, visit http://creativecommons.org/licenses/by-nc-nd/4.0/.

References

Belov DI, Armstrong RD (2011) Distributions of the Kullback–Leibler divergence with applications. British Journal of Mathematical and Statistical Psychology 64:291–309. https://doi.org/10.1348/000711010X522227

Bohle K, Fritzen CP (2003) Results obtained by minimising natural frequency and MAC-value errors of a plate model. Mechanical Systems and Signal Processing 17(1):55–64. https://doi.org/10.1006/mssp.2002.1539

Botev ZI, Grotowski JF, Kroese DP (2010) Kernel density estimation via diffusion

Brehm M, Zabel V, Bucher C (2010) An automatic mode pairing strategy using an enhanced modal assurance criterion based on modal strain energies. Journal of Sound and Vibration 329(25):5375–5392. https://doi.org/10.1016/j.jsv.2010.07.006

Brincker R, Zhang L, Andersen P (2001) Modal identification of output-only systems using frequency domain decomposition. Smart Materials and Structures 10(3)

Cabboi A, Magalhães F, Gentile C, Cunha Á (2017) Automated modal identification and tracking: application to an iron arch bridge. Structural Control and Health Monitoring 24(1). doi:https://doi.org/10.1002/stc.1854

Cawley P (1997) Quick inspection of large structures using low frequency ultrasound. Structural Health Monitoring- Current Status and Perspectives 529–540

Ceravolo R, Coletta G, Miraglia G, Palma F (2021) Statistical correlation between environmental time series and data from long-term monitoring of buildings. Mechanical Systems and Signal Processing 152. https://doi.org/10.1016/j.ymssp.2020.107460

Ceravolo R, Lenticchia E, Miraglia G, Scussolini L (2024) Improving the dynamic behaviour of historic buildings using experimental data: application to a Baroque church. Journal of Civil Structural Health Monitoring 1–20

Coccimiglio S, Miraglia G, Coletta G, Epicoco R, Ceravolo R (2023) Balanced Definition of Thresholds for Mode Tracking in a Long-Term Seismic Monitoring System. Geosciences (Switzerland) 13(12). doi:https://doi.org/10.3390/geosciences13120365

Cortes C, Vapnik V (1995) Support-vector networks. Machine Learning 20(3):273–297. https://doi.org/10.1007/BF00994018

Dederichs AC, Øiseth O (2024) A novel and near-automatic mode tracking algorithm for civil infrastructure. Journal of Sound and Vibration 573. https://doi.org/10.1016/j.jsv.2023.118217

Diord S, Magalhães F, Cunha Á, Caetano E, Martins N (2017) Automated modal tracking in a football stadium suspension roof for detection of structural changes. Structural Control and Health Monitoring 24(11). https://doi.org/10.1002/stc.2006

Ezekiel M (1930) Methods of Correlations Analysis. Wiley, Ed.)

Forbes C, Evans M, Hastings N, Peacock B (2011a) Logistic Distribution. In: Statistical Distributions. John Wiley \& Sons, p 127–130

Forbes C, Evans M, Hastings N, Peacock B (2011b) Lognormal Distribution. In: Statistical Distribution. John Wiley \& Sons, p 131–134

Forbes C, Evans M, Hastings N, Peacock B (2011c) Normal (Gaussian) Distribution. In: Statistical Distribution. John Wiley \& Sons, p 143–148

Forbes C, Evans M, Hastings N, Peacock B (2011d) Weibull Distribution. In: Statistical Distributions. John Wiley \& Sons, p 193–201

González WM, Boroschek RL (2020). Modal tracking on a building with a reduced number of sensors system. Conference Proceedings of the Society for Experimental Mechanics Series 39–46. https://doi.org/10.1007/978-3-030-12115-0_6

Kotsiantis SB, Zaharakis I, Pintelas P (2007) Supervised machine learning: a review of classification techniques. Emerging Artificial Intelligence Applications in Computer Engineering 160(1):3–24. & others.

Kullback S (1951) Kullback-Leibler divergence

Limongelli MP (2019a) Vibration-based structural health monitoring: challenges and opportunities. Advances in Engineering Materials, Structures and Systems: Innovations, Mechanics and Applications 1999–2004.

Limongelli MP (2019b) Vibration-based structural health monitoring: challenges and opportunities. Advances in Engineering Materials, Structures and Systems: Innovations, Mechanics and Applications 1999–2004

Magalhães F, Cunha Á, Caetano E (2009) Online automatic identification of the modal parameters of a long span arch bridge. Mechanical Systems and Signal Processing 23(2):316–329. https://doi.org/10.1016/j.ymssp.2008.05.003

Moser P, Moaveni B (2011) Environmental effects on the identified natural frequencies of the Dowling Hall Footbridge. Mechanical Systems and Signal Processing 25(7):2336–2357. https://doi.org/10.1016/j.ymssp.2011.03.005

Nicola Cavalagli GC, Ubertini F (2018) Earthquake-Induced Damage Detection in a Monumental Masonry Bell-Tower Using Long-Term Dynamic Monitoring Data. Journal of Earthquake Engineering 22(sup1):96–119. https://doi.org/10.1080/13632469.2017.1323048

Overschee P, Moor B (1996) Subspace Identification for Linear Systems. Kluwer Academic Publishers, Ed.)

Pereira S, Magalhães F, Gomes JP, Cunha Á (2022) Modal tracking under large environmental influence. Journal of Civil Structural Health Monitoring 12(1):179–190. https://doi.org/10.1007/s13349-021-00536-2

Rainieri C, Fabbrocino G, Manfredi G, Dolce M (2012) Robust output-only modal identification and monitoring of buildings in the presence of dynamic interactions for rapid post-earthquake emergency management. Engineering Structures 34:436–446. https://doi.org/10.1016/j.engstruct.2011.10.001

Reynolds D (2009) Gaussian Mixture Models *. Encyclopedia of Biometrics 714:(659–663)

Ruotolo R, Surace C (1997) Damage detection using singular value decomposition. DAMAS 97: Structural Damage Assessment Using Advanced Signal Processing 87–96

Scussolini L, Foti V, Civera M, Ceravolo R, Pistone G (2023). Redesign of Strengthening Interventions on Historical Buildings. The Case Study of an Earthquake-Damaged Bell Tower. International Conference on Experimental Vibration Analysis for Civil Engineering Structures 708–717

Sharma PK, Haleem H, Ahmad T (2015). Improving classification by outlier detection and removal. Emerging ICT for Bridging the Future-Proceedings of the 49th Annual Convention of the Computer Society of India CSI 2:621–628

Sivori D, Merani MGB, Bocchi F, Spina D, Cattari S (2024) Environmental effects on the experimental modal parameters of masonry buildings: experiences from the Italian Seismic Observatory of Structures (OSS) network. Journal of Civil Structural Health Monitoring https://doi.org/10.1007/s13349-024-00847-0

Sohn H, Worden K, Farrar CR (2002) Statistical damage classification under changing environmental and operational conditions. Journal of Intelligent Material Systems and Structures 13(9):561–574. https://doi.org/10.1106/104538902030904

Tallón-Ballesteros AJ, Riquelme JC (2014) Deleting or keeping outliers for classifier training? 2014 Sixth World Congress on Nature and Biologically Inspired Computing (Nabic 2014) 281–286

Torczon V (1997) On the convergence of Pattern Search Algorithms. SIAM Journal on Optimization 7(1):1–25. https://doi.org/10.1137/S1052623493250780

Ubertini F, Comanducci G, Cavalagli N (2016) Vibration-based structural health monitoring of a historic bell-tower using output-only measurements and multivariate statistical analysis. Structural Health Monitoring 15(4):438–457

Ubertini F, Comanducci G, Cavalagli N, Laura Pisello A, Luigi Materazzi A, Cotana F (2017) Environmental effects on natural frequencies of the San Pietro bell tower in Perugia, Italy, and their removal for structural performance assessment. Mechanical Systems and Signal Processing 82:307–322. https://doi.org/10.1016/j.ymssp.2016.05.025

Yang XM, Li H, Yi TH, Qu CX, Liu H (2022) Fully automated modal tracking for long-span high-speed railway bridges. Advances in Structural Engineering 25(16):3475–3491. https://doi.org/10.1177/13694332221130792

Publisher's Note Springer Nature remains neutral with regard to jurisdictional claims in published maps and institutional affiliations.

Authors and Affiliations

Stefania Coccimiglio[1] · Gaetano Miraglia[1,2] · Valeria Cavanni[1] · Alessio Crocetti[1,2] · Rosario Ceravolo[1,2]

✉ Stefania Coccimiglio
stefania.coccimiglio@polito.it

[1] Politecnico di Torino, Corso Duca degli Abruzzi, 24, 10129, Turin, Italy

[2] Responsible Risk Resilience interdepartmental Centre (R3C), Politecnico di Torino, Corso Duca degli Abruzzi, 24, 10129, Turin, Italy